molecular pharmaceutics

ARTICLE

pubs.acs.org/molecularpharmaceutics

In Vivo Labeling of B16 Melanoma Tumor Xenograft with a Thiol-Reactive Gadolinium Based MRI Contrast Agent

Valeria Menchise,[†] Giuseppe Digilio,[*,‡] Eliana Gianolio,[§] Evelina Cittadino,[§] Valeria Catanzaro,[§] Carla Carrera,[§] and Silvio Aime[§]

[†]Institute for Biostructures and Bioimages (CNR) c/o Molecular Biotechnology Center (University of Turin), Via Nizza 52, I-10126 Torino, Italy

[‡]Department of Environmental and Life Sciences, Università del Piemonte Orientale "A. Avogadro", Viale T. Michel 11, I-15121 Alessandria, Italy

[§]Department of Chemisty IFM & Center for Molecular Imaging, University of Turin, Via Nizza 52, I-10126 Torino, Italy

Supporting Information

ABSTRACT: Murine melanoma B16 cells display on the extracellular side of the plasma membrane a large number of reactive protein thiols (exofacial protein thiols, EPTs). These EPTs can be chemically labeled with Gd-DO3A-PDP, a Gd(III)-based MRI contrast agent bearing a 2-pyridinedithio chemical function for the recognition of EPTs. Uptake of gadolinium up to 10^9 Gd atoms per cell can be achieved. The treatment of B16 cells ex vivo with a reducing agent such as tris(2-carboxyethyl)phosphine (TCEP) results in an increase by 850% of available EPTs and an increase by 45% of Gd uptake. Blocking EPTs with *N*-ethylmaleimide (NEM) caused a decrease by 84% of available EPTs and a decrease by 55% of Gd uptake. The amount of Gd taken up by B16 cells is therefore dependent upon the availability of EPTs, whose actual level in turn changes according to the extracellular redox microenvironment. Then Gd-DO3A-PDP has been assessed for the labeling of tumor cells in vivo on B16.F10 melanoma tumor-bearing mice. Gd-DO3A-PDP (or Gd-DO3A as the control) has been injected directly into the tumor region at a dose level of 0.1 μmol and the signal enhancement in MR images followed over time. The washout kinetics of Gd-DO3A-PDP from tumor is very slow if compared to that of control Gd-DO3A, and 48 h post injection, the gadolinium-enhancement is still clearly visible. Therefore, B16 cells can be labeled ex vivo as well as in vivo according to a common EPTs-dependent route, provided that high levels of the thiol reactive probe can be delivered to the tumor.

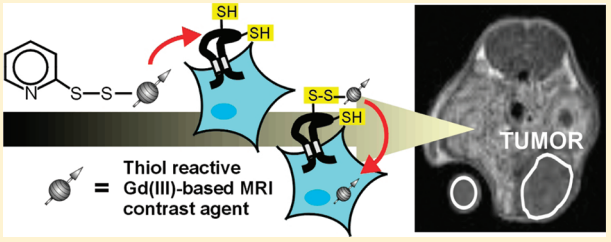

KEYWORDS: contrast agent, gadolinium, MRI, melanoma, microenvironment, redox, tumor

INTRODUCTION

Although solid tumors can have widely different cell/tissue origins and morphology, most of them share some physiologic and metabolic properties that concur to create the microenvironment where cancer cells can compete advantageously over surrounding noncancer cells and finally proliferate. Acidosis, hypoxia, increased metabolism, and abnormal perfusion typically define the tumor microenvironment.[1] Severe hypoxia and acidosis have been related to aggressive cell phenotype, poor clinical outcome, and low likelihood of patient survival.[2,3] A highly reducing microenvironment has been related to increased cancer cell proliferation[4−6] and resistance to radio- and chemotherapies.[7,8] Therefore, the characterization of the redox microenvironment around and within tumors is of great importance to evaluate the invasiveness of cancers, to predict resistance to radio- and chemotherapy, and for decision-making with regard to treatment. Several molecular imaging modalities and responsive probes are available for the imaging of the tumor microenvironment parameters such as tumor pH, energy metabolism, hypoxia, perfusion, and angiogenesis.[9−14] As the pO_2 levels in tumors are generally low, hypoxia is often used as an indirect evaluation of the tumor redox microenvironment.[15] The direct assessment of the tumor redox microenvironment is more challenging, as experimental difficulties arise in studying the tumor redox either in in vivo or in cultured cells,[16] resulting in a scarcity of suitable imaging probes. Imaging of hypoxia can be achieved by PET by means of the ^{18}F-FMISO redox sensitive tracer.[17−19] Tumor redox maps have also been achieved by electron paramagnetic resonance imaging (EPRI) by using nitroxide based spin-labels. These compounds are reduced within tumors to the diamagnetic (EPR silent) hydroxylamine forms at a rate dependent on the intracellular redox state of tumor cells, which is believed to be in turn influenced by hypoxia levels.[20] A manganese (II/III)−porphyrin complex has been proposed as a redox responsive probe for MRI.[21]

We are interested in finding new MRI methods for sensing the extracellular redox in tumors rather than the intracellular redox.

Received: March 3, 2011
Accepted: July 24, 2011
Revised: June 17, 2011
Published: July 25, 2011

Scheme 1. Chemical Structure of Gd-DO3A-PDP

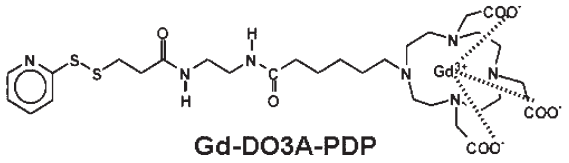

Within the cytoplasm of living cells, a strictly controlled, reducing environment is found that may change according to the cell phase (proliferation, differentiation/growth arrest, apoptosis).[22] The main redox buffer is represented by thiol/disulfide redox couples, mainly consisting of the cysteine containing γGlu-Cys-Gly tripeptide known as glutathione (GSH/GSSG), the thioredoxin system, and the protein thiols pool. Within the cytoplasm, thiols (including protein thiols) are favored over disulfide forms, resulting in a typical GSH/GSSG ratio greater than 30:1 and up to 100:1.[23,24] In the extracellular space, the redox environment is more oxidizing than in the cytoplasm and subjected to much larger magnitude and time fluctuations. Cysteine residues in proteins and other compounds are essentially under the disulfide form. The thiol groups from cysteine residues belonging to the extracellular domain of membrane proteins (exofacial protein thiols/disulfides, EPTs/EPDs) represent the boundary layer between the intra- and extracellular redox pools. The redox state of these groups and the EPTs/EPDs ratio is weakly coupled with the intracellular redox buffering systems, being therefore rather sensitive to the state of the extracellular milieu.[25,26] As a matter of fact, many mammalian cells contain chemically reactive EPTs at concentrations in the range of 1−60 nmol SH/10^6 cells (corresponding to 6×10^8 to 4×10^{10} EPTs/single cell), and fluctuations as large as 800% have been reported when exposing cells in vitro to oxidizing/reducing conditions.[27−30]

We have recently described a Gd(III)-DO3A based compound designed for ex vivo cell labeling applications.[27,31,32] This compound, named Gd-DO3A-PDP (Scheme 1), contains the 2-pyridinedithio group that can form disulfide bridges with the cell's EPTs. The Gd(III) chelate thus anchored on the cell surface is transported into the cytoplasm, and by this route as many as 1.2×10^{10} Gd(III) atoms have been shown to be internalized per single cell. The amount of internalized Gd(III) is dependent upon the availability of EPTs displayed by cells, which is believed to be in turn influenced by the extracellular redox microenvironment (the more reducing the microenvironment, the higher the EPTs level). As tumor cells are adapted to proliferate under hypoxia conditions, high levels of EPTs and an efficient labeling of cells are expected. To assess whether Gd-DO3A-PDP could be used to label tumors in vivo and to report about the redox microenvironment, murine melanoma B16.F10 cancer cells have first been assayed ex vitro for their ability to take up Gd-DO3A-PDP as a function of the EPTs levels. Then, Gd-DO3A-PDP has been delivered to tumor regions in mice grafted with a B16 melanoma derived tumor and the signal enhancement monitored over time has been compared to that obtained with control Gd-DO3A or to that found in nontumor tissues.

EXPERIMENTAL SECTION

Cell Cultures and in Vitro Labeling Experiments. The culture media RPMI 1640, biological buffers, and fetal bovine serum (FBS) were purchased from Cambrex, East Rutherford, NJ. All other supplements/chemicals were from Sigma Chemical Co., St Louis, MO, except TCEP (Pierce, Rockford, IL, USA).

About 8×10^5 mouse melanoma B16.F10 cells were seeded into a 4 cm diameter Petri dish and allowed to proliferate by further incubation for 24 h at 37 °C under CO_2−air (5:95) atmosphere in RPMI 1640 culture medium supplemented with 100 U/mL of penicillin, 100 U/mL of streptomycin, and 10% FBS. After this incubation time, cells typically reached a confluence of about 80%. The culture medium was removed and cells washed with isotonic HEPES buffer. Blocking/stimulation of the EPTs was then achieved by incubating cells for 15 min at 25 °C in a minimum medium (Earl's Balanced Salt Solution, EBSS, in which the phosphate has been replaced by 10 mM HEPES) containing either *N*-ethylmaleimide (NEM 50−200 μM) or tris(2-carboxyethyl)phosphine (TCEP, 100−1000 μM). After this reaction time, cells were carefully washed with HEPES buffer to remove excess chemicals and either assayed for EPTs or subjected to Gd uptake experiments. EPTs were titrated by the DTNB method as published elsewhere.[29,31] Shortly, cells were added in the Petri dish with 1 mL of HEPES buffer and DTNB was added to a final concentration of 200 μM. After 30 min incubation at room temperature, the supernatant was recovered and the 2-nitro-5-thiobenzoic acid released evaluated by measuring the absorbance at 412 nm ($\varepsilon = 14150\ M^{-1}\ cm^{-1}$). Gd uptake was evaluated by incubating cells for 2 h at 37 °C with 2 mM Gd-DO3A-PDP or Gd-DO3A as the control. Then the medium was removed and cells carefully washed to remove excess Gd complexes and recovered mechanically by harvesting them with a scraper. After recovering from the labeling medium, cells were suspended in 200 μL of HEPES and sonicated for 10 s to achieve complete lysis. A small aliquot of this homogenate (5 μL) was used to determine the total protein content by the Bradford method[33] using bovine serum albumin as the standard. Another aliquot (100 μL) of the homogenate was added with the same volume of HCl 37% and left at 120 °C overnight in a sealed vial. Upon this treatment, all Gd^{III} is released as the free aquo-ion, whose concentration can be determined by measuring the water relaxation time.[27,34] Relaxation rate measurements were performed at 20 MHz and 25 °C on a Spinmaster spectrometer (Stelar, Mede, Italy), by using a conventional inversion recovery pulse sequence. The obtained R_{1obs} data are related to the concentration of the paramagnetic species according to the formula:

$$R_{1obs} = R_{1W} + [Gd^{III}] \cdot r_{1p}^{Gd(III)}$$

where R_{1W} is the relaxation rate of pure water (0.38 s^{-1}) and $r_{1p}^{Gd(III)}$ the millimolar relaxivity of the Gd^{III} aquo-ion (13.5 $mM^{-1}\ s^{-1}$ in 6 M HCl, 25 °C). The moles of Gd^{III} obtained in this way were normalized against the weight (in milligrams) of cellular proteins. By considering that 1 mg of protein (Bradford) corresponds to 4.5×10^6 B16.F10 cells, the amount of gadolinium taken up can be expressed in terms of number of Gd atoms per single cell (Gd atom/cell). The detection limit of this assay is 1.0×10^8 Gd atom/cell. Uptake of Gd-DO3A was all the way below this limit.

Animal Models. Male C57Bl/6 mice (6−8 weeks of age) were obtained from Charles River Laboratories (Calco, Italy) and kept in standard housing with standard rodent chow and water available ad libitum and a 12 h light/dark cycle. Experiments were performed according to the national regulations and were

approved by the local animal experiments ethical committee. B16.F10 murine melanoma were cultured as monolayers at 37 °C in a 5% CO_2-containing humidified atmosphere in RPMI 1640 culture medium supplemented with 100 U/mL of penicillin, 100 U/mL of streptomycin, and 10% FBS. For tumor induction, 8×10^5 B16.F10 melanoma cells in 0.2 mL of PBS were inoculated subcutaneously (sc) in the right flank of C57Bl/6 mice. Around one week after B16.F10 injection, mice developed a solid tumor of 5−8 mm in diameter and were used for imaging evaluation.

In Vivo MRI. Prior to the acquisition of MR images, mice were anesthetized by injecting a mixture of 20 mg/kg tiletamine/zolazepam (Zoletil 100; Virbac, Milan, Italy) and 5 mg/kg xylazine (Rompun; Bayer, Milan, Italy). Intratumor and intramuscular administration of Gd complexes were done by injecting 10 μL of 12 mM solutions in PBS (corresponding to 0.12 μmol of CA). Gd-DO3A and Gd-HPDO3A (ProHance, Bracco, Milan, Italy) were kindly provided as a gift by Bracco Imaging (Colleretto Giacosa, TO, Italy). The synthesis and full characterization of Gd-DO3A-PDP is described in ref 27. Intravenous injections of the CA were done trough a catheter placed in the tail vein (200 μL of 10 mM solution of the CA in saline, corresponding to a dose of 0.1 mmol/kg). MR images after intratumor or intramuscular administration of the CA were acquired at 1 T by means of an Aspect M2 high performance MRI system (Aspect Magnet Technologies Ltd., Netanya, Israel), mounting a NdFeB permanent magnet with a field homogeneity of 0.2−0.5 gauss. This system is equipped with a 35 mm solenoid Tx/Tr coil (inner diameter 35 mm) and fast gradient coils (gradient strength, 450 mT/m at 60 A; ramp time, 250 μs at 160 V). MR images were acquired using a standard T_1-weighted multislice spin echo sequence, with a flip angle of 90°, TR/TE/NEX 250/8/10, FOV = 4.0 cm × 4.0 cm, data matrix 128 × 128, slice thickness 1 mm, 17 slices. MR images after iv administration of Gd-DO3A-PDP and related controls were acquired at 7 T on a Bruker Avance300 NMR spectrometer equipped with a microimaging probe (birdcage resonator with 10 mm inner diameter). Images were acquired with a standard T_1-weighted multislice multiecho fat-suppressed sequence with a flip angle of 90°, TR/TE/NEX = 250/3.2/6, FOV 3.0 × 3.0 cm, data matrix 128 × 128, 5 slices each having 1.0 mm thickness.

The mean signal intensity (SI) values was calculated on a region of interest (ROI) manually drawn on the whole tumor and/or muscle and averaged over three adjacent slices. The mean SI measured was normalized against a standard Gd solution (reference). The mean SI enhancement (% signal enhancement, SE%) was calculated according to the following equation:

$$SE\% = \frac{I_{POST} - I_{PRE}}{I_{PRE}} \times 100$$

where I_{PRE} and I_{POST} are the MR signal intensity (both normalized with respect to the SI of the external reference) before and after the injection of the CA. The SE is expressed as percentage normalized by the SE measured at $t = 0$, representing the time at which the first postcontrast image has been taken.

RESULTS

In Vitro Labeling of B16 Cells. Mouse melanoma B16.F10 cells have been characterized in vitro to assess the dynamic range of EPTs levels that these cells can reach while being still viable. Therefore EPTs on cell membranes have been counted by means of the DTNB assay[29] after exposing cells to either a thiol blocking group (we used the cell impermeable *N*-ethylmaleimide, NEM) or a reducing agent (we used tris(2-carboxyethyl)phosphine, TCEP). The viability of B16 cells subjected to incubation with NEM up to 200 μM or TCEP up to 1000 μM was >85% under all circumstances. EPTs levels span almost 2 orders of magnitude, in between the lower limit of 3.7×10^8 EPT/cell (corresponding to treatment with 200 μM NEM) and the upper limit of 2.9×10^{10} EPT/cell (corresponding to treatment with 1000 μM TCEP). This confirms that the EPTs level promptly responds to both extracellular stimuli (Figure 1). The EPTs level following the treatment with TCEP increases proportionally with the concentration of the reducing agent in the culture medium. An increase of EPTs as large as 850% with respect to control can be found for the maximum concentration of TCEP used, without appreciable signs of cell damage. On the other hand, the decrease of EPTs due to reaction with NEM goes to −84% at 50 μM NEM, and beyond this concentration there is no further decrease of EPTs, while some sign of cell damage starts to be detected.

Next we assessed the relationship between the number of EPTs displayed by cells and the extent of labeling that can be achieved by means of the Gd-DO3A-PDP label. Melanoma cells

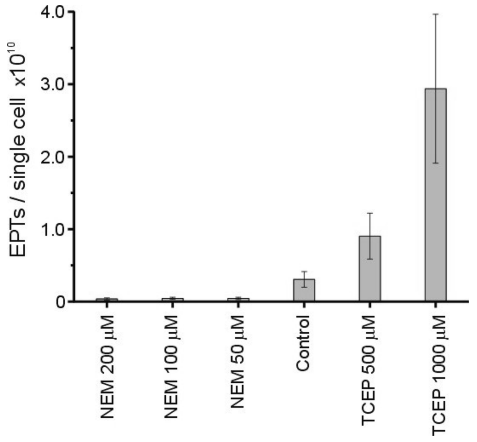

Figure 1. Level of EPTs (expressed as number of EPTs per single cell) displayed by B16 cells in response to the treatment with NEM and TCEP.

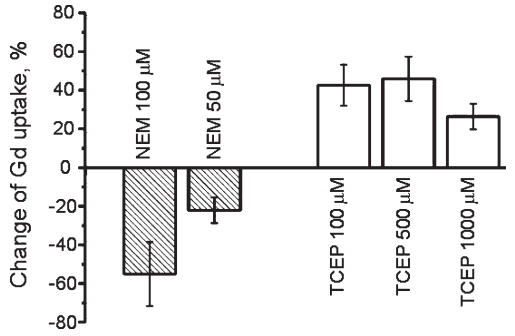

Figure 2. Uptake of Gd-DO3A-PDP by B16.F10 melanoma cells treated with either TCEP or NEM (to stimulate or block exofacial protein thiols, respectively) as compared to untreated cells. Uptake of the Gd complex is given as the percentage relative to controls (i.e., cells that were not exposed to NEM/TCEP). Hatched bars: cells pretreated with NEM (EPTs blocked). White bars: cells pretreated with TCEP (EPTs stimulated).

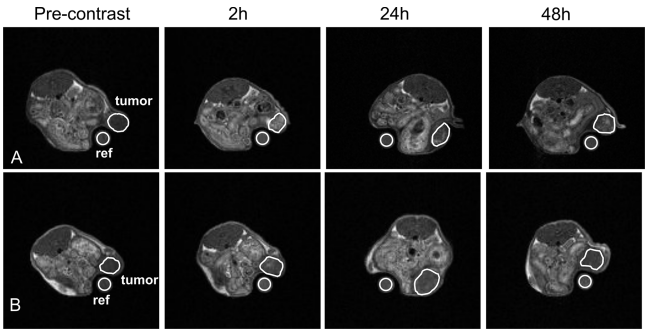

Figure 3. T_{1w}-SE axial images at 1 T (TR/TE/NEX 250/8/10) of mice subcutaneously grafted with a B16 tumor. The ROIs used to measure the signal enhancement in tumor is shown. Time course of the signal enhancement from precontrast to 48 h post intratumor injection (at 0.12 μmol) of (A) Gd-DO3A-PDP; (B) Gd-DO3A.

adhering to the floor of culture dishes (confluence of 80%) were preincubated with either NEM or TCEP (15 min, 25 °C) to decrease/increase the availability of EPTs, the excess of the EPT modifier carefully washed away, and cells were finally incubated with the Gd(III) label (2 h, 2 mM, 37 °C). After further extensive washings, the total amount of Gd(III) taken up by cells was determined by the relaxometric method.[27,34] As shown in Figure 2, there is a correlation between the level of EPTs and Gd uptake, as the extent of labeling is larger by 45% when cells are pretreated with TCEP (100−500 μM) with respect to untreated controls and is lower by 55% when cells are pretreated with 100 μM NEM. The relationship between the level of EPTs and Gd(III) uptake is not linear: although the level of EPTs steadily increases with the concentration of TCEP (from 9.0×10^9 EPTs/cell at 500 μM TCEP to 2.9×10^{10} EPTs/cell at 1000 μM TCEP), the uptake of Gd levels off at about 2×10^9 Gd/cell just after treatment with 100 μM TCEP (Figure 2). The nontrivial relationship linking the expected levels of EPTs with the extent of Gd labeling is due to the fact that, after chemical modification of the chemical status of EPTs, the cell machinery will operate to restore the physiologic surface thiols/disulfide redox balance. In our experimental setup, EPTs are first blocked/stimulated, then the excess of chemicals (TCEP/NEM) carefully washed out, and finally cells are incubated again with Gd-DO3A-PDP typically up to two hours. By those washing/incubation times, a substantial rescue of blocked EPTs or oxidation back to disulfide forms can occur. Note that cells can not be incubated simultaneously with both the Gd probe and the chemical EPT modifiers because direct cross reactivity between the probe and those chemicals might occur.

In Vivo Labeling of B16 Cells Xenografted into Mice. A cohort of 12 C57B1/6 mice was subcutaneously injected with 8×10^5 B16.F10 melanoma cells in the right flank. Animals were subjected to MRI when the tumor size reached a diameter of 5−8 mm, a condition typically achieved in 7−10 days after inoculation of tumor cells. These animals were divided into four groups for treatment with either Gd-DO3A-PDP (intratumor/intramuscle) or Gd-DO3A (intratumor/intramuscle). In the first group (n = 4), T_1-weighted spin−echo MR axial images were acquired before and after intratumor injection of 0.1 μmol (5 μmol/kg) of the contrast agent, and the signal enhancement in the tumor measured over a time lapse of 3000 min (ca. 48 h). A representative series of MR images of the mouse before and after treatment with Gd-DO3A-PDP is shown in Figure 3. As

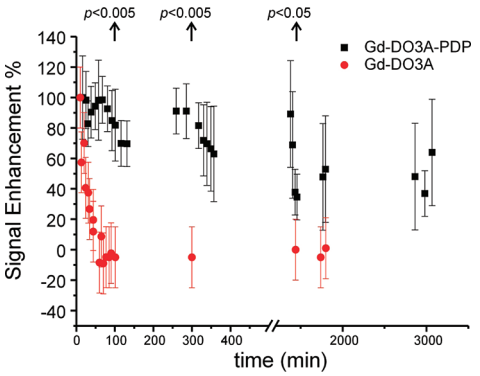

Figure 4. Time course of the signal enhancement (SE%) in the tumor region measured after direct intratumor injection (0.12 μmol) of Gd-DO3A-PDP (squares) or control Gd-DO3A (circles). The SE is expressed as percentage normalized by the SE measured at t = 0, representing the time at which the first postcontrast image has been taken. For Gd-DO3A-PDP, each point is the average from 4 mice; for Gd-DO3A, each point is the average of 3 mice. Error bars represent ± SD. Arrows indicate Student's t test statistical analysis at selected time points (100, 300, and 1400 min).

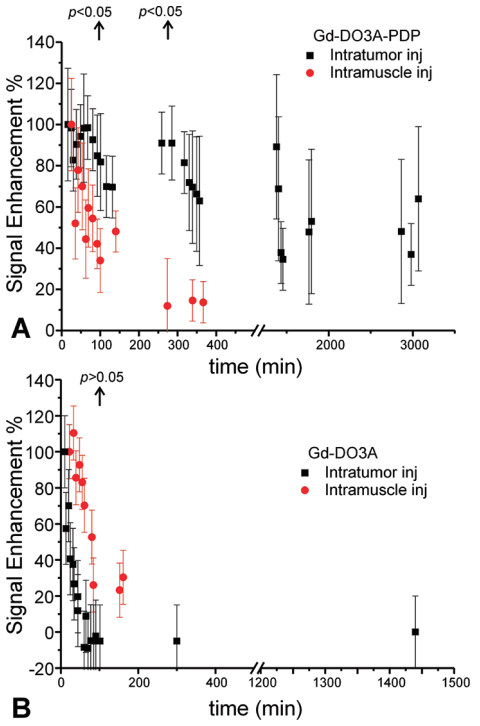

Figure 5. Comparison of the decay of SE in the tumor or in the muscle after injection of Gd complexes. (A) Gd-DO3A-PDP: SE in the tumor area after intratumor injection (squares, average of 4 mice) and SE in the muscle after intramuscular injection (circles, average of 3 mice). (B) Gd-DO3A: SE in the tumor area after intratumor injection (squares, average over 3 mice) and SE in the muscle after intramuscular injection (circles, average over 2 mice). Error bars represent ± SD. Arrows indicate Student's t test statistical analysis at selected time points.

the control, the second group (n = 3) of tumor bearing mice was injected within the tumor mass with Gd-DO3A at the same dose. The signal enhancement (SE) in the tumor remains very high and almost constant over time for Gd-DO3A-PDP, being

still as much as about 50% after 48 h (Figure 4). For Gd-DO3A, a much steeper decrease of the signal intensity is observed, with SE decaying to zero after one hour. Thus, Gd-DO3A-PDP is much more efficiently retained within the tumor microenvironment than Gd-DO3A. Because the molecular sizes and physicochemical properties of Gd-DO3A-PDP and Gd-DO3A are quite similar, the observed large difference between their tumor washout kinetics can not be accounted for in terms of diffusion/permeation differences. To assess whether the enhanced retention of Gd-DO3A-PDP is tumor specific, the third and fourth groups of tumor bearing animals were intramuscularly injected with either Gd-DO3A-PDP or Gd-DO3A (n = 3 and n = 2, respectively) on the left hind leg that was not hosting the tumor, and the signal enhancement in the muscle was monitored over time. The washout kinetics of Gd-DO3A-PDP from muscle is much faster than from the tumor, the former being essentially completed after about 200 min (Figure 5A). On the other hand, the washout of Gd-DO3A from muscle or tumor have similar kinetics (Figure 5B), and the enhancement of the decay vanishes within 200 min. We also note that the washout kinetics of Gd-DO3A-PDP and Gd-DO3A from muscle are essentially superimposable. Taken together, these findings indicate that the enhanced retention of Gd-DO3A-PDP within the tumor is due to specific molecular interactions between the Gd-DO3A-PDP probe and the tumor microenvironment.

When Gd-DO3A-PDP was injected intravenously (at a dose of 0.1 mmol/kg) via a catheter in the tail vein, the SE detected in the tumor region reached a maximum shortly after bolus injection, followed by a fast decay (Supporting Information S1). The maximum signal enhancement and the kinetics of the signal enhancement were very similar to those of control Gd-DO3A. This indicates that Gd-DO3A-PDP can diffuse from the bloodstream into the tumor area but not in a form available for the labeling of EPTs.

DISCUSSION

In vitro labeling experiments showed that B16 melanoma cells can accumulate large amounts of Gd-DO3A-PDP and that the extent of Gd uptake can be modulated by the level of EPTs displayed by cells (the higher the level, the higher the uptake). This modulation stems from the fact that labeling with Gd-DO3A-PDP relies primarily upon the formation of a disulfide bridge between the Gd complex and cell surface thiols, followed by the transport of the membrane bound Gd complex within the cytoplasm through active cellular processes.[27] Dynamic contrast enhancement MRI data in vivo clearly show that Gd-DO3A-PDP has a greatly enhanced retention time in the tumor with respect to the untargeted control Gd-DO3A and that retention of Gd-DO3A-PDP is enhanced in tumor but not in muscle. The longer retention time within the tumor microenvironment is in line with the preferential internalization of Gd-DO3A-PDP into tumor cells.[35]

Internalization is only seen when Gd-DO3A-PDP is directly injected into the tumor, whereas poor uptake and short retention times are seen when the compound is administered systemically. This difference can be explained by considering that a concentrated bolus of the intact probe can be delivered to EPT displaying cells by direct intratumor injection, whereas a small fraction of intact Gd-DO3A-PDP can diffuse into the tumor through the systemic route. Most of the Gd-DO3A-PDP probe, once injected into the bloodstream, is exposed to the many blood pool free thiols. Although the redox environment in plasma favors disulfide forms over free thiols, the total concentration of low molecular free thiols (including cysteine, glutathione, cysteinylglycine, and homocysteine) can be still as high as 15 μM.[22,36,37] Protein thiols (most notably cys34 of serum albumin, but also those of blood cells and even blood vessel walls) are also known to be rather abundant and to bind thiol reactive compounds,[3,38,39] thus contributing substantially to the deactivation of Gd-DO3A-PDP before it could reach the tumor microenvironment. Poor labeling of tumors after iv injection cannot be ascribed to insufficient permeation of the Gd complex within the tumor microenvironment because MRI images show an increase of the SE shortly after iv administration of the probe (comparable to that of control Gd-DO3A). However, the residence time within the tumor after iv injection should be rather short, preventing an efficient coupling with EPTs. Thus the complex enters the tumor, but not in the chemical form and concentration that are needed to label cells. The failure of systemically administered Gd-DO3A-PDP to label tumor cells can be taken as an indirect evidence about the necessity of a prompt chemical reaction between the thiol reactive probe and the EPTs.

In summary, melanoma tumor cells can be labeled ex vivo as well as in vivo (under the form of a xenografted tumor) according to a common EPT-dependent mechanism, provided that high levels of the "intact" thiol reactive probe can be delivered to the tumor cells. The uptake of the Gd-chelate increases with increasing EPT levels, namely when the extracellular redox microenvironment gets more reducing. In vitro, a reducing microenvironment can be modeled by incubating cells with a number of reducing chemical agents, including free thiols, such that the level of EPTs can be increased by 1 order of magnitude.[27,28,30] In vivo, hypoxia is believed to be the main determinant for highly reducing conditions around tumor cells. As a result, high EPT levels might be regarded as a marker of hypoxia. From this perspective, the EPT-dependent labeling of cells could be in principle exploited to map hypoxia within tumors. However, it must be emphasized that the MRI signal enhancement due to the accumulation of gadolinium within different tumor regions would be a function of at least two variables, namely the local concentration of EPTs and the local concentration of the thiol reactive probe. Thus, to translate contrast enhancement maps into redox maps, the relative weight of each of the two variables on contrast enhancement should be quantitatively assessed first.

ASSOCIATED CONTENT

Supporting Information. Time course of the gadolinium enhancement in tumors after intravenous injection of Gd-DO3A-PDP or Gd-DO3A. This material is available free of charge via the Internet at http://pubs.acs.org.

AUTHOR INFORMATION

Corresponding Author

*Department of Environmental and Life Sciences (DISAV), Università del Piemonte Orientale "A. Avogadro", V.le T. Michel 11, 15121-Alessandria (AL), Italy. Phone: + 39 0131 360371. Fax: + 39 0131 360250. E-mail: giuseppe.digilio@mfn.unipmn.it.

■ ACKNOWLEDGMENT

We gratefully acknowledge Dr. Cinzia Boffa for technical assistance. Economic and scientific support from EC-FP6-projects DiMI (LSHB-CT-2005-512146), MEDITRANS (Targeted Delivery of Nanomedicine: NMP4-CT-2006-026668), EU-FP7-HEALTH-2007-1.2-4 ENCITE (European Network for Cell Imaging and Tracking Expertise), EU-COST D38 Action, and Regione Piemonte (Ricerca Sanitaria Finalizzata 2008bis and PIIMDMT projects) is gratefully acknowledged.

■ REFERENCES

(1) Gatenby, R. A.; Gillies, R. J. Why do cancers have high aerobic glycolysis? *Nature Rev.* **2004**, *4*, 891–899.

(2) Rofstad, E. K. Microenvironment-induced cancer metastasis. *Int. J. Radiat. Biol.* **2000**, *76*, 589–605.

(3) Raghunand, N.; Jagadish, B.; Trouard, T. P.; Galons, J.-P.; Gillies, R. J.; Mash, E. A. Redox-Sensitive Contrast Agents for MRI Based on Reversible Binding of Thiols to Serum Albumin. *Magn. Reson. Med.* **2006**, *55*, 1272–1280.

(4) Jonas, C. R.; Ziegler, T. R.; Gu, L. H.; Jones, D. P. Extracellular thiol/disulfide redox state affects proliferation rate in a human colon carcinoma (Caco2) cell line. *Free Radical Biol. Med.* **2002**, *33*, 1499–1506.

(5) Jonas, C. R.; Gu, L. H.; Nkabyo, Y. S.; Mannery, Y. O.; Avissar, N. E.; Sax, H. C.; Jones, D. P.; Ziegler, T. R. Glutamine and KGF each regulate extracellular thiol/disulfide redox and enhance proliferation in Caco-2 cells. *Am. J. Physiol.* **2003**, *285*, R1421–R1429.

(6) Rehman, F.; Shanmugasundaram, P.; Schrey, M. P. Fenretinide stimulates redox-sensitive ceramide production in breast cancer cells: potential role in drug-induced cytotoxicity. *Br. J. Cancer* **2004**, *91*, 1821–1828.

(7) Prezioso, J. A.; Shields, D.; Wang, N.; Rosenstein, M. Role of gamma-glutamyltranspeptidase-mediated glutathione transport on the radiosensitivity of B16 melanoma variant cell lines. *Int. J. Radiat. Oncol. Biol. Phys.* **1994**, *30*, 373–381.

(8) Paolicchi, A.; Lorenzini, E.; Perego, P.; Supino, R.; Zunino, F.; Comporti, M.; Pompella, A. Extracellular thiol metabolism in clones of human metastatic melanoma with different gamma-glutamyl transpeptidase expression: implications for cell response to platinum-based drugs. *Int. J. Cancer* **2002**, *97*, 740–745.

(9) Glunde, K.; Gillies, R. J.; Neeman, M.; Bhujwalla, Z. M. In: *Molecular Imaging: Principles and Practice*; Weissleder R., Ross, B. D., Rehemtulla, A., Gambhir, S. S., Eds .; PMPH-USA: Beijing, 2010; pp 844−863.

(10) Glunde, K.; Pathak, A. P.; Bhujwalla, Z. M. Molecular-functional imaging of cancer: to image and imagine. *Trends Mol. Med.* **2007**, *13* (7), 287–297.

(11) Penet, M.-F.; Pathak, A. P.; Raman, V; Ballesteros, P.; Artemov, D.; Bhujwalla, Z. M. Noninvasive Multiparametric Imaging of Metastasis-Permissive Microenvironments in a Human Prostate Cancer Xenograft. *Cancer Res.* **2009**, *69* (22), 8822–8829.

(12) Neeman, M.; Provenzale, J. M.; Dewhirst, M. W. Magnetic Resonance Imaging Applications in the Evaluation of Tumor Anglogenesis. *Semin. Radiat. Oncol.* **2001**, *11* (1), 70–82.

(13) Bhujwalla, Z. M.; Artemov, D.; Ballesteros, P.; Cerdan, S.; Gillies, R. J.; Solaiyappan, M. Combined vascular and extracellular pH imaging of solid tumors. *NMR Biomed.* **2002**, *15*, 114–119.

(14) Garcìa-Espinosa, M. A.; Rodrigues, T. B.; Sierra, A.; Benito, M.; Fonseca, C.; Gray, H. L.; Bartnik, B. L.; Garcìa-Martìn, M. L.; Ballesteros, P.; Cerdán, S. Cerebral glucose metabolism and the glutamine cycle as detected by in vivo and in vitro 13C NMR spectroscopy. *Neurochem. Int.* **2004**, *45*, 297–303.

(15) Manzoor, A. A.; Yuan, H.; Palmer, G. M.; Viglianti, B. L.; Dewhirst, M. K. In *Molecular Imaging: Principles and Practice*; Weissleder R., Ross, B. D., Rehemtulla, A., Gambhir, S. S., Eds.; PMPH-USA: Beijing, 2010; pp 756−780.

(16) Cook, J. A.; Gius, D.; Wink, D. A.; Krishna, M. C.; Russo, A.; Mitchell, J. B. Oxidative stress, redox, and the tumor microenvironment. *Semin. Radiat. Oncol.* **2004**, *14*, 259–266.

(17) Groves, A. M.; Win, T.; Ben Haim, S.; Ell, P. J. Non-[18F]FDG PET in clinical oncology. *Lancet Oncol.* **2007**, *8*, 822–830.

(18) Rischin, D.; Hicks, R. J.; Fisher, R.; Binns, D.; Corry, J.; Porceddu, S.; Peters, L. J. Prognostic Significance of [^{18}F]-Misonidazole Positron Emission Tomography-Detected Tumor Hypoxia in Patients With Advanced Head and Neck Cancer Randomly Assigned to Chemoradiation With or Without Tirapazamine: A Substudy of Trans-Tasman Radiation Oncology Group Study 98.02. *J. Clin. Oncol.* **2006**, *24*, 2098–2104.

(19) Eschmann, S. M.; Paulsen, F.; Reimold, M.; Dittmann, H.; Welz, S.; Reischl, G.; Machulla, H. J.; Bares, R. Prognostic impact of hypoxia imaging with 18F-misonidazole PET in non-small cell lung cancer and head and neck cancer before radiotherapy. *J. Nucl. Med.* **2005**, *46* (2), 253–260.

(20) Hyodo, F.; Soule, B. P.; Matsumoto, K.-I.; Matsumoto, S.; Cook, J. A.; Hyodo, E.; Sowers, A. L.; Krishna, M. C.; Mitchell, J. B. Assessment of tissue redox status using metabolic responsive contrast agents and magnetic resonance Imaging. *J. Pharm. Pharmacol.* **2008**, *60* (8), 1049–1060.

(21) Aime, S.; Botta, M.; Gianolio, E.; Terreno, E. A pO_2-Responsive MRI contrast agent based on the redox switch of manganese(II/III)−porphyrin complexes. *Angew. Chem., Int. Ed.* **2000**, *39*, 747–750.

(22) Moriarty-Craige, S. E.; Jones, D. P. Extracellular thiols and thiol/disulphide redox in metabolism. *Annu. Rev. Nutr.* **2004**, *24*, 481–509.

(23) Schafer, F. Q.; Buettner, G. R. Redox environment of the cell as viewed through the redox state of the glutathione disulfide/glutathione couple. *Free Radical Biol. Med.* **2001**, *30* (11), 1191–1212.

(24) Ghezzi, P. Oxidoreduction of protein thiols in redox regulation. *Biochem. Soc. Trans.* **2005**, *33*, 1378–1381.

(25) Sahaf, B.; Heydari, K.; Herzenberg, L. A.; Herzenberg, L.A. Lymphocyte surface thiol levels. *Proc. Natl. Acad. Sci. U.S.A.* **2003**, *100*, 4001–4005.

(26) Sahaf, B.; Heydari, K.; Herzenberg, L. A.; Herzenberg, L. A. The extracellular microenvironment plays a key role in regulating the redox status of cell surface proteins in HIV-infected subjects. *Arch. Biochem. Biophys.* **2005**, *434*, 26–32.

(27) Digilio, G.; Menchise, V.; Gianolio, E.; Catanzaro, V.; Carrera, C.; Napolitano, R.; Fedeli, F.; Aime, S. Exofacial protein thiols as a route for the internalization of Gd(III)-based complexes for MRI cell labelling. *J. Med. Chem.* **2010**, *53*, 4877–4890.

(28) Laragione, T.; Gianazza, E.; Tonelli, R.; Bigini, P.; Mennini, T.; Casoni, F.; Massignan, T.; Bonetto, V.; Ghezzi, P. Regulation of redox-sensitive exofacial protein thiols in CHO cells. *Biol. Chem.* **2006**, *387*, 1371–1376.

(29) Jiang, X.-M.; Fitzgerald, M.; Grant, C. M.; Hogg, P. J. Redox Control of Exofacial Protein Thiols/Disulfides by Protein Disulfide Isomerase. *J. Biol. Chem.* **1999**, *274*, 2416–2423.

(30) Laragione, T.; Bonetto, V.; Casoni, F.; Massignan, T.; Bianchi, G.; Gianazza, E.; Ghezzi, P. Redox regulation of surface protein thiols: identification of integrin α-4 as a molecular target by using redox proteomics. *Proc. Natl. Acad. Sci. U.S.A.* **2003**, *100*, 14737–14741.

(31) Digilio, G.; Catanzaro, V.; Fedeli, F.; Gianolio, E.; Menchise, V.; Napolitano, R.; Gringeri, C.; Aime, S. Targeting exofacial protein thiols with GdIII complexes. An efficient procedure for MRI cell labelling. *Chem. Commun.* **2009**, 893–895.

(32) Carrera, C.; Digilio, G.; Baroni, S.; Burgio, D.; Consol, S.; Fedeli, F.; Longo, D.; Mortillaro, A.; Aime, S. Synthesis and characterization of a Gd(III) based contrast agent responsive to thiol containing compounds. *Dalton Trans.* **2007**, 4980–4987.

(33) Bradford, M. M. A rapid and sensitive method for the quantitation of microgram quantities of protein utilizing the principle of protein−dye binding. *Anal. Biochem.* **1976**, *72*, 248–254.

(34) Geninatti Crich, S.; Biancone, L.; Cantaluppi, V.; Duò, D.; Esposito, G.; Russo, S.; Camussi, G.; Aime, S. Improved route for the

visualization of stem cells labeled with a Gd-/Eu-chelate as dual (MRI and fluorescence) agent. *Magn. Reson. Med.* **2004**, *51*, 938–944.

(35) Geninatti Crich, S.; Cabella, C.; Barge, A.; Belfiore, S.; Ghirelli, C.; Lattuada, L.; Lanzardo, S.; Mortillaro, A.; Tei, L.; Visigalli, M.; Forni, G.; Aime, S. In vitro and in vivo magnetic resonance detection of tumor cells by targeting glutamine transporters with Gd-based probes. *J. Med. Chem.* **2006**, *49*, 4926–4936.

(36) Deneke, S. M. Thiol-based antioxidants. *Curr. Top. Cell. Regul.* **2001**, *36*, 151–180.

(37) Andersson, A.; Lendgren, A.; Hultberg, B. Effect of thiol oxidation and thiol export from erythrocytes on determination of redox status of homocysteine and other thiols in plasma from healthy subjects and patients with cerebral infarction. *Clin. Chem.* **1995**, *41*, 361–366.

(38) Peters, T. Jr. *All about Albumin; Biochemistry, Genetics and Medical Applications*; Academic Press: London, 1996.

(39) Raghunand, N.; Guntle, G. P.; Gokhale, V.; Nichol, G. S.; Mash, E. A.; Jagadish, B. Design, synthesis, and evaluation of 1,4,7,10-tetra-azacyclododecane-1,4,7-triacetic acid derived, redox-sensitive contrast agents for magnetic resonance imaging. *J. Med. Chem.* **2010**, *53*, 6747–6757.